Microfiltration and ultrafiltration as a post-treatment of biogas plant digestates for producing concentrated fertilizers

Camilleri Rumbau, Maria Salud; Norddahl, Birgir; Wei, Jiang; Christensen, Knud Villy; Fjerbæk Søtoft, Lene

Published in:
Desalination and Water Treatment

DOI:
10.1080/19443994.2014.989638

Publication date:
2015

Document version:
Accepted manuscript

Microfiltration and ultrafiltration as a posttreatment of biogas plant digestates for producing concentrated fertilizers

M.S. Camilleri-Rumbau[1,*]; B. Norddahl[1]; J. Wei[2]; K.V. Christensen[1], L.F. Søtoft[1]

(1) Department of Chemical Engineering, Biotechnology and Environmental Technology –University of Southern Denmark, Niels Bohrs Allé 1, 5230 Odense M, DK

(2) Alfa Laval Nakskov A/S, Business Centre Membranes, Stavangervej 10, 4900 Nakskov, DK

* Corresponding author: mscr@kbm.sdu.dk (Maria Salud Camilleri-Rumbau)

Keywords: microfiltration, ultrafiltration, digested manure, polysulphone (PS), polyvinylidene fluoride (PVDF), polyethersulphone (PES), phosphorus recovery, zeta potential

Abstract

Biogas plant digestate liquid fractions from biogas plants can be concentrated by microfiltration and ultrafiltration. Two types of microfiltration membranes (polysulphone (PS) and surface modified polyvinylidene fluoride (PVDF)) were used to process digestate liquid fractions, and to assess their applicability in the recovery of particulate phosphorus compared to an ultrafiltration membrane (polyethersulphone (PES)). Results show that membrane material, operational conditions and pore diameter influenced the permeate flux pattern during microfiltration. The PS membranes initially had a higher tendency to foul than PVDF membranes. However, during the filtration process, as fouling built up, the permeate flux behaviour of the two membranes became very similar. During the concentration of digestate liquid fractions, the microfiltration PS membrane and the ultrafiltration PES membrane achieved the highest phosphorus rejection (80 % w/w.), suggesting that there was a correlation between the membrane material and both the fouling trend and phosphorus rejection. A two-step basic-acidic cleaning was unable to recover the initial water flux for the fouled microfiltration membranes. In conclusion, the PS microfiltration membranes might be a good strategy for recovering phosphorus from digestate liquid fractions. Further research leading to

adequate cleaning procedures for microfiltration PS and PVDF membranes treating digestate liquid fractions though are needed.

Introduction

Livestock production has increased dramatically in the last decades due to an increased consumption in meat and an increase in the human population [1]. As large centralized livestock production leads to large production of manure, centralized biogas production by anaerobic digestion is of growing interest as a green energy solution in areas with industrialized livestock production. Anaerobic digestion stabilizes and converts about 20-25% of the organic matter present in animal manure into biogas; it is considered a reliable source of bioenergy and it minimizes greenhouse gas (GHG) emissions and odors [2-4]. Anaerobic digestion mineralizes some of the organic nitrogen and increases the NH_3/NH_4^+ content by about 15%. The same occurs with the organic phosphorous, the concentration of which in the inorganic form also increases after anaerobic digestion [4]. Digestates contain large amounts of nutrients in the form of nitrogen, phosphorus, potassium, organic matter and micronutrients (e.g. calcium, chloride, sodium, copper, zinc, manganese, etc.) [5]. It is common practice to use digestates as a fertilizer source and to spread the resulting liquid fraction after solid-liquid separation on the fields [6]. However, this can lead to environmental problems mostly related to NH_3 volatilization as well as surface and groundwater eutrophication [1, 7]. Moreover, digestates present an unbalanced distribution of nutrients with respect to crop uptake and demand, which makes their application as reliable fertilizers difficult.

When digestates from centralized biogas plants are applied as fertilizer to fields far away from the biogas plant, it is advantageous to separate digestate in a solid fraction rich in phosphorus and a liquid fraction rich in nitrogen and potassium [8], but low in phosphorus. Separation in a solid and liquid fraction both reduces transportation costs and makes it possible to obtain a more balanced fertilizer composition. Traditionally, this separation is done using either a decanter centrifuge or a

screw press. The obtained liquid fractions though are still dilute in nitrogen and potassium and further concentration of these nutrients is necessary [1]. Moreover, the concentration of particulate phosphorus present in the liquid fraction might be increased by concentration of the particulate dry matter or total solids content. It is estimated that 20 % of the phosphorus in digestates is present in the fraction below 0.45 μm, while the remaining 30% has been found in particulates larger than 10 μm. Especially, the particle range between 0.45 and 10 μm, is of interest as it is the fraction that contains approximately 50% of the total phosphorus in the digestate [1, 9].

Several studies have already proved that membrane separation is suitable for concentrating digestate liquid fractions [2, 10-12]. Microfiltration has proved to be a reliable technique for treating digestate liquid fractions and removing suspended solids from the liquid stream [10]. Ultrafiltration has also proved to be suitable for further removal of suspended solids and colloids [12]. However, there are only few studies on microfiltration and ultrafiltration of digestate liquid fractions with special focus on the influence of membrane material, operating conditions and pore size on membrane fouling and phosphorus recovery [11-17]. In this study, the fouling tendency of PS and surface modified PVDF membranes was investigated. The influence of membrane surface hydrophilicity on membrane fouling has previously been studied by Wei et al [18]. They showed that, during filtration of BSA (bovine serum albumin), membranes made of hydrophobic materials such as PS or PES caused severe fouling compared to membranes made of more hydrophilic surfaces (e.g. surface modified PVDF). Beier et al. [19] investigated the effect of static adsorption during ultrafiltration of an amylase enzyme solution. They found that the PES membrane had a larger static adsorption of macromolecules, due to its hydrophobic nature, than the surface modified PVDF. Other studies, focused on the influence of the ionic strength and solution pH on the adsorption of proteins on membrane surfaces. For instance, Bayramoglu et al and Li et al [20, 21] found that proteins with opposite surface charge compared to that of the membrane, presented the strongest adsorption. Li et al. also found [21] that, although convective forces tended to increase the amount

of foulant accumulated near the membrane surface, electrostatic interactions played a stronger role, which was evident from the resulting irreversible adsorption. Thus, controlling electrostatic interactions could reduce adsorption of foulants onto the membrane and consequently reduce long-term membrane fouling. Membrane surface charge has been used as a parameter for investigating the membrane fouling tendency during ultrafiltration of silica particles [22] and during microfiltration of egg protein [23], chlorolignin and whey protein [24] among other studies mentioned by Deshmukh et al [25]. However, the majority of these studies only involved rather limited solution chemistries and none of them was related to filtration of digestate liquid fractions. It has though been showed that when microfiltration membranes are used in ammonia removal for pig slurry by membrane distillation, the surface charge influences fouling [26]. Therefore, investigating the effect of surface charges of the membrane-digestate liquid fraction system is relevant to understand better the fouling mechanism in these types of membrane-based processes. This can be done by monitoring the electrostatic interaction between membrane and foulant [27, 28]. The most common technique for evaluating the membrane surface charge is by streaming potential [27, 29]. The zeta potential, estimated from the Helmholtz-Smoluchowsky equation from the streaming potential, has been used as an index of the surface charge and applied during the characterization of membrane materials [27, 29, 30], although it is used in terms of apparent or observed zeta potential, as the Helmholtz-Smoluchowsky equation neglects the effect of surface conductance. The observed zeta potential thus becomes a preliminary diagnostic tool to identify a potential cause of membrane fouling [25].

In this study, the fouling tendency of surface modified PVDF and PS membranes was investigated based on the observed zeta potential and operational conditions in order to evaluate the interaction between the membrane material and the feed. Phosphorus rejection during membrane filtration was also investigated. As an alternative to phosphorus recovery by microfiltration, the usage of a commercial setup combining ultrafiltration directly with an anaerobic digester was also introduced.

However, the study of the fouling characteristics and filtration performance of the ultrafiltration system is only included for comparison. It is not the objective of this paper.

Materials

Biogas plant digestates

Microfiltration experiments were carried out on the anaerobic digestate liquid fraction from Fangel Biogas (Odense, Denmark). The feed to the anaerobic digester consisted of approximately 50% of pig slurry, 15% cattle manure, 10% chicken manure and 25% food waste. The anaerobic digestion was mesophilic (39-40^{o}C) and the hydraulic retention time was 30 days. The final digestate was centrifuged via a decanter centrifuge (AD-1220, GEA Westfalia, Germany). The obtained solid fraction is normally composted while the liquid fraction is distributed to local farmers and used as a liquid fertilizer. Fangel biogas plant treats 260 tonnes·day^{-1} of animal slurry and 60 tonnes·day^{-1} of industrial food waste. This allows an annual energy production of 16-18 million kWh·year^{-1}. The digestate liquid fraction obtained after centrifugation was sieved using a 2-step manual sieve (Retsch 5657, Germany) of 350 and 125 µm mesh size. The resulting sieved liquid fraction was used as feed to the microfiltration unit. The composition and characteristics of the digestate liquid fraction used as feed to the microfiltration system is shown in Table 1.

The ultrafiltration experiments were carried out at Bioscan A/S' anaerobic digester ultrafiltration pilot plant at mesophilic conditions (35°C) and at a hydraulic retention time of 12 days. The concentrate was recirculated to the digester [13]. The digestate had a pH of 8 and a composition of 3.2% total solids; 2.7 (g·L^{-1}) of total ammoniacal nitrogen (TAN); 0.53 g·L^{-1} of phosphorus and 0.46 g·L^{-1} of potassium.

Filtration setups

Microfiltration unit

The microfiltration experiments were carried out on a LabStak® M10 laboratory plant (Alfa Laval, Denmark) (Figure 1). The M10 is a cross flow filtration module with an active membrane area of 0.036 m^2 which can accommodate four membrane flat sheets (see Table 2). The laboratory plant had three M10 membrane modules placed in parallel. This made it possible to test three different membrane pore sizes at nearly identical operational conditions. The feed was pumped from one shared 15L-feed tank through an external spur gear pump (GC6-KDT-KKU, Pulsafeeder Inc. USA) with a maximum flow rate of 2.8 $m^3 \cdot h^{-1}$. Piping and connections in the plant were made of stainless steel AISI 316. The inflow velocity to the microfiltration module was measured through a digital flowmeter (IFS1000K, Krohne Altometer, Germany) and the transmembrane pressure by analogue pressure gauges P1 and P2 (see Figure 1) (Tempress, Denmark). The temperature was controlled through a multitube heat exchanger (Alfa Laval, Sweden). All the experiments were run at 30°C, chosen as a relevant temperature for mesophillic digestate liquid fractions obtained after digestate centrifugation.

Ultrafiltration unit

The ultrafiltration experiments were performed by Bioscan A/S (Denmark) at their pilot plant (Figure 2) unit. PES tubular membranes (STUF 2.5/1.7 AL (S) 719, Membratek, South Africa) having an active area of 7.1 m^2 and a cut-off of 40 kDa. The system was run at 1.5-3.5 bar and a cross flow velocity of 2, 2.6, 2.9 and 4.3 $m \cdot s^{-1}$.

The anaerobic digester was fed with screw-press pre-treated slurry from a pig farm. The digestate was produced in the 150 L pilot scale digester tank. The digestion temperature was kept constant at 35°C by an external heating system. All piping was made of AISI 304 stainless steel. The digested biomass was separated and treated subsequently by tubular ultrafiltration membranes. The digestate velocity to the UF module was controlled by a calibrated screw pump (Mono S32M, Mono Pumps, UK) with a VLT® frequency converter (Danfoss, Denmark). The bulk of the ultrafiltration

permeate was recirculated into the digester in order to keep the liquid level constant in the digester [14].

Methods

Microfiltration experimental procedure

Two membrane materials (surface modified PVDF and PS) and three pore sizes (0.2, 0.5 and 0.8 µm) were tested (Table 2). The PVDF membrane surface was modified by the manufacturer to increase its hydrophilicity. Fresh membranes were used for each experimental run. Membrane pre-cleaning and conditioning was done with 0.1% w/w Ultrasil (Henkel) solution at 50^{o}C recirculated for 30 minutes.

The feed was tested at constant feed velocities of 1.1 and 1.4 m·s^{-1} and constant transmembrane pressures of 1.0 and 1.5 bar. The feed temperature was kept at 30^{o}C throughout the entire set of experiments. Before starting a filtration cycle, clean water tests were performed on the fresh membranes, using deionized water at the same operational conditions as the related filtration experiment. Each filtration experiment lasted 3-4 h. Following, another clean water test was performed in order to compare the permeate flux before and after filtration of the digestate liquid fraction. Then the membranes were chemically cleaned. The cleaning procedure was a sequence of a basic cleaning using a 0.1 M NaOH solution (pH 12.1 ± 0.1), followed by an acidic cleaning using 0.1 M citric acid solution (pH 2.2 ± 0.1). Each cleaning was conducted for 30 minutes at 30^{o}C. In between the basic and acidic cleaning cycles, clean water tests were performed to check the membrane flux recovery after each chemical cleaning step. The cleaning procedure was done at the same operational conditions as the corresponding filtration experiments.

Surface characterization of membranes and materials

Surface charge of particulate matter in Fangel Biogas digestate and microfiltration fractions

169 The observed zeta potential of the Fangel Biogas digestate, concentrate and permeate fractions
170 after microfiltration were obtained using Electrophoretic Light Scattering (Zetasizer Nano, Malvern,
171 UK). The sample dispersant was water and the analysis temperature 25^{o}C. The scattering angle was
172 12.8^{o} and the samples were analysed in a disposable Z-dip cell. The zeta potential calculation from
173 experimental electrokinetic data follows the Helmholtz-Smoluchowski equation. All the samples
174 required dilution. The observed zeta potential and standard deviation were reported as an average
175 of at least 12 readings. Measurements were done in triplicate.

176 *Surface charge of microfiltration PVDF and PS membrane surfaces*

177 A Surpass adjustable gap cell (Anton Paar, Austria) for small rectangular pieces of planar samples
178 was used to obtain the observed zeta potential by measuring the streaming potential of the PS and
179 PVDF membrane samples. Prior to the measurements, membrane samples were cleaned to remove
180 the glycerine protective coating on the membrane surface. 0.03 wt% NaOH was used for pre-treating
181 PVDF membranes and 0.3 wt% NaOH was used for PS membranes. The membrane samples were
182 fixed on the sample holders with double-sided adhesive tape. The cell gap, where two pieces of 2x1
183 mm membrane sample were attached, had a height of 0.1mm. Before performing the first
184 measurement, the complete electrolyte circuit was rinsed carefully with deionized water. A 500 mL
185 solution of 1mM NaCl was used as electrolyte and the pressure drop along the gap was set at 300
186 mbar [28]. The pH was controlled by adding HCl 0.1 M and NaOH 0.1 M to the 1mM NaCl feed
187 solution. The streaming potential per unit pressure, through and on the membrane surface, was
188 evaluated at a constant Cl^- concentration of 1 mM with a gradual substitution of protons by Na^+ [31].

189 ***Analytical methods***

190 *Chemical analysis*

191 During the microfiltration experiments, the pH was measured with a pHM83 pHmeter (Radiometer
192 Analytical, France). The dry matter (DM) or total solids content was measured with a HG63 Halogen
193 Moisture Analyzer (Mettler Toledo, Sweden). TKN and TAN were measured by the Kjeldahl method
194 [32] using a Tecator Digester block and a Kjeltec Distillation unit (Foss, Denmark). Values for
195 phosphorus (P), potassium (K^+), calcium (Ca^{2+}), magnesium (Mg^{2+}), sodium (Na^+) and chlorine (Cl^-)
196 were analyzed by ICP-OES (ICAP 6500 Duo, Thermo Scientific, USA). For the ICP-OES analysis, 0.1g of
197 each sample was weighed and introduced in a digestion Teflon tube of an Ultraclave Microwave
198 Digester (Milestone Inc., USA) and acidic digestion was allowed by adding 4mL of HNO_3 PA-ISO 69%
199 and 1mL of H_2O_2 33% to the digestion tube. The temperature was set to increase from room
200 temperature to 220°C over a period of 20 minutes. Once the samples were cooled down, the
201 digestion Teflon tubes were filled up to 25mL with deionized water (Merck Millipore, Germany) and
202 the samples were analyzed by ICP-OES.

203 *Data analysis*

204 Microfiltration data is presented in terms of relative permeate flux, i.e. the absolute permeate flux
205 related to the initial water flux for each tested membrane (J/J_0) (Eq. 1). The reasoning behind this is
206 that new fresh membranes were used for each experimental run and a high standard deviation of
207 the related clean water fluxes was observed due to the variations during membrane production. This
208 makes it difficult to carry out a direct water flux comparison between different operational
209 conditions difficult. By treating the data as elative permeate fluxes, data is standardized and a direct
210 comparison among the obtained values during the microfiltration experiments can be done.

211 $$Relative\ permeate\ flux = \frac{J}{J_0} \quad \text{(Eq. 1)}$$

212 Where J ($L \cdot m^{-2} \cdot h^{-1}$) is the permeate flux and J_0 ($L \cdot m^{-2} \cdot h^{-1}$) is the initial water flux obtained for each
213 fresh membrane before starting the filtration experiment. To compare the relative permeate fluxes

of paired experiments, scatter plots are used. The comparison time trace line generated is then compared to the identity line y = x. If the relative permeate flux of the membranes or effect of experimental conditions on the relative permeate flux are identical, the time trace line should fall approximately along the identity line. Linear interpolation between data points was used to compare relative fluxes at the same processing time when experimental data at identical processing times were not available.

Results and discussion

Determination of the surface charge of liquid fractions and microfiltration membranes

The composition of the polymeric membrane active layer influences the surface charge density of the membrane. The same applies for the particulates of the Fangel Biogas digestate liquid fraction, concentrate and permeate obtained from the microfiltration. As membrane foulant interactions are a major issue during microfiltration of particulate liquid samples [22] such as digestate liquid fractions, the observed zeta potential of PVDF (PVDF2 and PVDF5) and PS membranes (PS2 and PS5) were measured as a function of pH. This is crucial for understanding the acid-base properties of membrane surface functional groups. Measuring the observed zeta potential of the feed as well as for the obtained concentrates and permeates (Table 3) would help to elucidate the interaction between the foulant and the microfiltration membrane surfaces.

Table 3 presents the observed zeta potential of the feed, concentrate and permeate samples obtained during concentration experiments using PS5 and PVDF5. The typical pH of biogas plant digestates is 8 to 8.5. All samples were measured at a pH of 8.2 ± 0.1, to simulate the typical feed pH. All the tested samples had a zeta potential between -18.2 and -14.7 mV. These negative zeta potential values at high pH are most likely related to the amino and carboxyl groups present in the proteins of the analyzed samples and only to a smaller degree to the charge of the solids [33]. This

might explain why feed, concentrate and permeate show similar zeta potentials, as proteins are not expected to be separated to a significant degree by microfiltration.

Figure 3 presents the zeta potential measurements for PVDF and PS membranes as a function of the solution pH. For the studied pH range, the PS membranes showed a significantly less negative zeta potential than the surface modified PVDF membranes. In the pH range of interest for the membrane feed (pH 8-8.5), both PS and PVDF membrane materials showed stable values of observed zeta potentials being -18.2mV and -16.0 for and PVDF2 and PVDF5, respectively; and -6.9mV and -7.1mV for PS2 and PS5, respectively. The initial properties of the membranes suggest that foulants might get more attracted to the PS membrane surface rather than to the PVDF membrane as the feed has an observed zeta potential of about -18mV at a basic pH (Table 3). As the difference in charge is larger between foulants and the PS than for the PVDF membrane, the PS membrane is thus less repulsive initially.

Microfiltration of digestate liquid fraction during full recycling experiments

Water test on microfiltration membranes

Water tests were conducted on fresh membranes prior to each filtration experiment (Table 4). As expected, flux increased with the applied transmembrane pressure following Darcy's law. However, a large difference between each new membrane was observed, making conclusions based on the clean water flux alone difficult. The influence of the cross flow velocity was unclear although during water tests this should not have a high impact (i.e. absence of fouling). It is characteristic for all water tests, except perhaps for the PS5, that the increase in cross flow velocity leads to a lower flux at a similar transmembrane pressure. Differences in membrane compaction cannot be the cause as both transmembrane pressure and cross flow velocity were maintained constant and the transmembrane pressure did not increase with increasing cross flow velocity. Due to these variations in clean water fluxes between each new documented membrane, results during microfiltration of

digestate liquid fractions were evaluated in terms of relative permeate fluxes following Eq. 1.

Microfiltration performance: Effect of operational conditions, material interaction and membrane pore size

Figure 4 presents the permeate fluxes obtained with experimental time for the studied PVDF and PS membranes during microfiltration of digestate liquid fraction. As can be observed, for the two PVDF and PS membranes, the obtained permeate fluxes are very low compared to the clean water fluxes (Table 4) for the same testing conditions. Moreover, a severe permeate flux decline is observed immediately during the start-up of the filtration cycle. This behaviour has been reported previously to be caused by both concentration polarization and fouling on the membrane surface [19], which are especially severe when treating digestate liquid fractions. An increase in the feed cross flow velocity during microfiltration also increased the permeate flux for all membranes. This might indicate the formation of concentration polarization and a reversible fouling layer that could be removed when increasing turbulence at the membrane surface [34]. Furthermore, the combination of a higher pressure (1.5bar) and lower cross flow velocity (1.1 $m \cdot s^{-1}$) resulted in the lowest permeate fluxes for all membranes probably due to a significant increase in the cake layer resistance. This behaviour is most likely caused by an increasing compression of the cake layer, as suggested by Razi et al. [34], as increasing the cross flow velocities to 1.4 $m \cdot s^{-1}$ did not lead to the same relative flux as measured at 1 bar.

The relative permeate fluxes (J/J_0) to compare the effect of membrane material and pore diameter during microfiltration using the two PS and PVDF membranes were plotted against each other in scatter plots (Figure 5 - Figure 7). These plots mostly give information about the effect of operational conditions on the relative permeate flux pattern. The reason why the relative permeate flux for PS is higher than the ones for PVDF is basically due to the higher clean water flux values obtained for PVDF membranes.

285 The impact of the operational conditions, i.e. applied pressure and cross flow velocity, on the
286 relative permeate fluxes for the same pore size, for the two PS and PVDF membranes can be
287 observed in the individual graphs in Figure 5 a), b) and c). The relative permeate flux achieved with
288 the PS membranes was generally higher than that obtained when using the PVDF membranes for a
289 similar filtration time (i.e. the time track lines lay beneath the identity line). However, it can be
290 observed that the relative permeate flux decay with time was more pronounced for PS membranes
291 than for PVDF membranes for all the membrane pore sizes. The application of a higher pressure also
292 affected the relative permeate flux of the PS membranes more negatively than the PVDF
293 membranes, and enhanced the reduction of the relative permeate flux most probably due to an
294 increasing compression of the cake layer, especially for the smaller membrane pore sizes (i.e. 0.2 µm
295 and 0.5 µm). The combination of low pressures and high velocities appeared to be beneficial for all
296 membranes. It also seems that the larger the membrane pore size, the smaller the effect of the
297 material interaction, which causes an ultimate similar permeate relative fluxes for the two PS and
298 PVDF membranes (Figure 4).

299 For the PVDF membranes (Figure 6), the relative fluxes were higher when using 0.5 and 0.8 µm
300 membrane pore diameters (Figure 6 b), c)) than for the 0.2 µm pore diameter membranes (Figure 6
301 a)). The increase in cross flow velocity led to a higher improvement in relative flux for the PVDF8
302 membrane than for the PVDF5 membrane (Figure 6 c)). Further, this trend is more pronounced at
303 lower than at higher pressure. This situation has two implications as i) the increase in shear force,
304 related to higher velocities, enhanced the removal of the loosely deposited particles on PVDF
305 membranes leading to an increase in the critical flux [22] and ii) the increase in pressure more
306 negatively affected the relative permeate flux of the membranes with the larger pore diameters.
307 This suggests that an increase in pressure causes more membrane blocking in the larger membrane
308 pores of the PVDF membranes [35].

Figure 7 shows the effect of PS membrane pore sizes on the relative permeate flux. It can be observed that the effect of material interaction was more pronounced for smaller pore sizes in PS membranes (Figure 7 a) and b)) especially for the experiments run at a lower pressure. An increase in pressure negatively affected the relative permeate flux on PS membranes. This most probably is due to an increasing compression in the cake layer, especially for smaller membrane pore sizes (0.2 µm and 0.5 µm). In contrast, an increase in the cross flow velocity affected positively the relative permeate flux of the PS membranes. However, this improvement was limited as compared to PVDF membranes, as foulants were strongly adsorbed on the PS membrane surfaces. The relative permeate fluxes achieved with the PS2 membranes were higher compared to the PS5 and PS8. However, the relative permeate flux values for both PS5 and PS8 were very alike (Figure 7 c). This suggests that for smaller pore sizes, the fouling mechanism related to PS membranes might be predominantly governed by the presence of an adsorbed layer that might enhance pore blocking and cake filtration for larger pore sizes.

Summary of microfiltration experiments

The PS membranes achieved a lower permeate flux than the PVDF membranes during approximately the first hour of the microfiltration experiment (shown in Figure 4), which suggests that material interaction initially plays an important role during microfiltration of digestate liquid fractions. The lower initial permeate flux for the PS membranes could be further explained by the fact that the PS membrane surface is more hydrophobic than the surface modified PVDF membrane [18, 19]. Additionally, the PS membrane surfaces present a less negative zeta potential (Figure 3) than the foulants (Table 3) and therefore were initially more prone to foul. For the PVDF membranes, membrane and feed zeta potentials (Figure 3) were comparable (Table 3) and hence initially the foulants were repulsed. During filtration, as fouling builds up, the membrane zeta potential becomes less important and the similar cake layer formed [19, 36] for the two PS and PVDF membranes, limits the permeate flux behaviour. This situation shows that, although the material interaction plays a

major role at the beginning of the filtration process, the morphology and composition of the fouling layer are the dominant factors controlling the permeate flux pattern during the microfiltration of digestate liquid fractions.

Microfiltration of digestate liquid fraction during concentration experiments

Batch concentration experiments were carried out on PVDF5 and PS5 membranes. During feed volume reduction, the total solid or dry matter concentration increased in the concentrate as did the total phosphorus content in the concentrate. The volume reduction is expressed by the volume reduction factor (VRF), defined as in Eq. 2.

$$VRF = \frac{V_P}{V_0} \quad \text{(Eq. 2)}$$

where

V_P: Volume of permeate collected (L)

V_0: Initial feed volume of feed (L)

Figure 8 shows the relative permeate flux decline with the increasing VRF. The flux behaviour during the concentration experiments was similar to what was observed during microfiltration at constant feed concentration (Figure 4) for both PVDF and PS membranes at similar operational conditions (1.4 $m \cdot s^{-1}$ and 1 bar). For the PVDF membrane, the relative permeate flux dropped 39% when the total solids content increased from 2.3 up to 4% (Table 5). The decrease in relative permeate flux for the PS membrane was 31% when the total solids increased from 2.5 to 3.9% (Table 5). For both membranes, the decrease in relative flux can be considered identical within the experimental error. A decrease in critical permeate flux has also been related to an increase in particle concentration [22]. In general, the flux decline during the concentration process was found to be more acute for PVDF membranes than for PS membranes as for the full recycling microfiltration experiments. This was also observed during full recycling filtration (Figure 4) and as explained, it is the initial difference

357 in zeta potential between the feed and the membrane material that determines the permeate flux
358 decay pattern [12], as the initial higher resistance to fouling for the PVDF membrane is negated by a
359 slower cake layer build up which finally equalizes the morphology and composition of the fouling
360 layers on the two PS and PVDF membranes.

361 ***Ultrafiltration of digestate liquid fraction during concentration experiments***

362 Ultrafiltration can be used as an alternative to microfiltration for concentration of particulate
363 phosphorous. As an alternative PES ultrafiltration membranes were used during the concentration
364 experiment carried out on the Bioscan A/S (Denmark) plant for determining their capacity to reject
365 phosphorus. Figure 9 shows a clear relationship between the increase in the volume reduction factor
366 (VRF) together with the increase in total solids in the concentrate and the decline in permeate flux.
367 As the total solids concentration increased, the flux decay became more acute being reduced by
368 more than 50% at a VRF 0.7 and 3.3 bar of applied pressure. During concentration, permeate flux
369 decline is thus a consequence of both fouling layer build up and concentration polarization [19].
370 Moreover, increases in osmotic pressure could also affect the driving force for the permeate flux as
371 the retentate concentration increases.

372 ***Phosphorus rejection during concentration experiments***

373 Figure 10 shows the phosphorus rejection achieved with PVDF, PS and PES membranes. The
374 phosphorus rejection was found to be higher for the PS5 microfiltration membrane (82% w/w) than
375 for the PVDF5 membrane (60% w/w) for the same VRF. By extrapolation, the PES membrane and the
376 PVDF5 membrane seemed to achieve a similar phosphorus rejection. This might be another indicator
377 that the membrane material did have a significant influence on the phosphorus rejection. Most likely
378 a tighter cake layer builts up on the PS membrane than on the PVDF membrane. This could lead to a
379 higher retention of fine particles by the PS than the PVDF. A counter argument to this explanation
380 would be that the PES and the PVDF show similar rejection, but as the ultrafiltration system used in

this study was constructed specifically to reduce the particulate matter, in principle to about 100%, the particle size distribution in the ultrafiltration feed setup was significantly different from that for the microfiltration membranes at similar VRF. It can be concluded that a similar retention is achieved for the ultrafiltration setup and the PVDF microfiltration membrane although making a direct comparison of the two systems is difficult. However, as a similar or better phosphorous retention is possible using microfiltration compared to ultrafiltration, microfiltration might be a cheaper alternative option.

Chemical analysis of the obtained fractions during concentration experiments

While the permeate flux decline during microfiltration and ultrafiltration concentration of digestate liquid fractions is severe, it is by no means detrimental. However, if the concentration of digestate liquid fractions is to be of practical interest, a substantial concentration of phosphorus should also be achieved. Table 5 shows the nutrient distribution between the concentrate and permeate fractions as a function of VRF. Total phosphorus is mainly attached to particles with a diameter between 0.45 and 10 µm [9] which are mostly retained by microfiltration and ultrafiltration. Thus, as the total phosphorus content in the concentrate is directly related to the total solids content, the phosphorus concentration in the retentate increased with increasing VRF. For similar reasons the phosphorus concentration in all permeate fractions was nearly constant during the concentration experiments. The phosphorus that could penetrate to the permeate side might be either in dissolved form or attached to particles small enough to pass through the fouling cake layer and membrane pores. As most of the nitrogen and potassium was present in dissolved form, the distribution of nitrogen and potassium was not affected to the same degree by the increase in total solids in the concentrate and thus the increase in VRF.

Cleaning of fouled microfiltration membranes

Membrane cleaning was applied to recover the membrane initial permeate flux after microfiltration of digestate liquid fractions. A simple two-step basic and acidic cleaning procedure was tested. The basic cleaning (0.1M NaOH, pH 12.1 ± 0.1) was intended to remove organic matter while the acidic cleaning (0.1M citric acid, pH 2.2 ± 0.1) would remove inorganic foulants. The cleaning procedures were performed after 3-4 hours of microfiltration of the digestate liquid fraction in full recycling mode. Table 6 shows the clean water flux recovery achieved after chemical cleaning compared to the clean water flux measured after the fouling cycle.

As can be observed in Table 6, the clean water flux recovery is insufficient for both fouled PVDF and PS membranes. The water flux recovery after a two-step basic-acidic chemical cleaning was 42% for PS membranes and 20% for PVDF membranes. However the clean water flux recovery after basic cleaning was 19% for PS and 33% for PVDF. This indicates that the acidic cleaning might not be a good strategy for PVDF membranes. Additionally, after flushing the membranes with water, PS membranes achieved 75% of water flux recovery while PVDF membranes reached 84%, compared to the respective final permeate flux value obtained at the end of the filtration cycle. Beier *et al* found [19] that after ultrafiltration of a model bovine serum albumin (BSA) solution, the initial water flux for PVDF membranes could be easily restored by flushing the membrane surface with water, while PS membranes required chemical cleaning. The reason for a better flux recovery achieved for PVDF membranes in this study could be related to the stronger attachment of the fouling layer to the PS membrane. This made necessary the chemical cleaning of the PS membrane to restore the initial water flux. Further investigations on PS and PVDF membranes fouled with digestate liquid fractions are necessary as the two membranes would need to undergo different cleaning strategies, rather than the ones performed in this paper, to achieve higher flux recoveries as obtained elsewhere [12].

Conclusions

Two types of microfiltration membranes (PS and surface modified PVDF), used to process digestate liquid fractions, were compared to an ultrafiltration membrane (PES) in terms of recovery of particulate phosphorus from biogas plant digestates. It was shown that the membrane material influences both the fouling mechanism and the rate of phosphorus recovery. When comparing the two microfiltration materials used in this study, it was found that the PS membranes form a fouling cake layer faster than PVDF membranes but as fouling starts to build up, the permeate flux of the two membranes becomes similar. The PS membranes presented a higher initial fouling than the PVDF membranes possibly due to a less negative zeta potential, which tended to initially attract foulants more. On one hand, at lower pore sizes for PS membranes, the formation of an adsorbed layer seems to play the main role during fouling while adsorption combined with pore blocking and a cake layer formation seems to rule the fouling mechanism at larger PS membrane pore sizes. On the other hand, PVDF membranes reached higher permeate fluxes for larger pore sizes. Moreover, increases in the applied pressure affected more negatively PS membranes than PVDF membranes in terms of the relative permeate flux, most probably due to cake layer compression, especially for smaller membrane pore sizes. Although membrane pore blocking could be enhanced with an increasing filtration pressure for larger pore sizes of PVDF membranes, increases in cross flow velocity affected more positively the permeate flux on the PVDF membranes than the PS membranes, as foulants were adsorbed stronger on the PS membrane surface. In general, larger membrane pore sizes (i.e. 0.5 µm and 0.8 µm pore size) for the two PS and PVDF membranes reduced the material effect on the fouling mechanism. Additionally, it was shown that when using PS and PES membranes a phosphorus recovery of about 80% was achieved while 60% phosphorus recovery was obtained when using PVDF membranes.

It is concluded that PS membranes could be a promising membrane material for phosphorus recovery from digestate liquid fractions, although further investigations on more suitable membrane cleaning procedures are necessary to improve the performance of this process.

Acknowledgments

The authors would like to thank Bioscan A/S, Fangel Biogas and Alfa Laval Nakskov for their support by providing digestate samples, facilities and scientific input, respectively. Special thanks to Mads Koustrup Jørgensen (Aalborg University) and Denis Okhrimenko (University of Copenhagen), for their guidance and input during the zeta potential measurements. Thanks to Hanne V. Hemmingsen (University of Southern Denmark) and to the Ionomic Laboratory (CEBAS, Spain) for chemical analysis of the microfiltration fractions.

The research leading to these results has received funding from the People Programme (Marie Curie Actions) of the European Union's Seventh Framework Programme FP7/2007-2013/ under REA grant agreement n° [289887].

List of tables and figures

Table 1: Composition of Fangel Biogas Plant digestate liquid fraction

PARAMETER	FANGEL BIOGAS DIGESTATE LIQUID FRACTION (used for microfiltration experiments)
pH	8.1-8.3
Dry matter (DM) (%)	2.7
Total Kjeldahl Nitrogen (TKN) ($g \cdot L^{-1}$)	3.4
Total Ammoniacal Nitrogen (TAN) ($g \cdot L^{-1}$)	3.15
Total Phosphorus (TP) ($g \cdot L^{-1}$)	0.46
Potassium (K^+) ($g \cdot L^{-1}$)	2.03
Calcium (Ca^{2+}) ($g \cdot L^{-1}$)	0.59
Magnesium (Mg^{2+}) ($g \cdot L^{-1}$)	0.09
Sodium (Na^+) ($g \cdot L^{-1}$)	1.28

Table 2: Membrane materials and experimental conditions during microfiltration experiments

ITEM	Microfiltration parameters
Membrane type	Flat sheet membranes
Membrane materials	Surface modified PVDF and PS

Manufacturer	Alfa Laval, Denmark
Mean pore diameters (µm)	0.2 (membrane types PVDF2, PS2) 0.5 (membrane types PVDF5, PS5) 0.8 (membrane types PVDF8, PS8)
Membrane area (m^2)	0.144
Operating transmembrane pressures (bar)	1 and 1.5
Feed flow ($L \cdot h^{-1}$)	800 and 1040
Operating feed cross flow velocity ($m \cdot s^{-1}$)	1.1 and 1.4
Operating Temperature (^oC)	30

Table 3: Observed zeta potential for samples obtained during concentration experiments reaching a volume reduction factor (VRF) of 0.5 approximately (SD: standard deviation)

Sample	Membrane type	Membrane material and mean pore diameter (µm)	Dilution	Observed zeta $potential_{average}$ (mV)	$SD_{average}$ (mV)
Feed			1:50	-18	6
Concentrate	PVDF5	PVDF 0.5	1:100	- 15	6
Concentrate	PS5	PS 0.5	1:50	- 15	6
Permeate	PVDF5	PVDF 0.5	1:50	- 17	7
Permeate	PS5	PS 0.5	1:50	- 16	7

Table 4: Water flux values for PVDF and PS membranes as a function of transmembrane pressure (ΔP) (1 and 1.5 bar) at different cross flow velocities (1.1. and 1.4 $m \cdot s^{-1}$)

Conditions		**Membrane type** **Water flux ($L \cdot m^{-2} \cdot h^{-1}$) × 10^3**					
v (m/s)	**ΔP (bar)**	**PVDF2**	**PVDF5**	**PVDF8**	**PS2**	**PS5**	**PS8**
1.4	1.50	2.27	1.38	2.63	0.65	1.51	1.02
1.4	1.00	1.13	0.95	0.96	0.31	0.55	0.52
1.1	1.50	2.50	1.35	2.94	0.61	1.28	1.41
1.1	1.00	2.17	1.19	2.27	0.32	0.76	0.70

Table 5: Nutrient distribution during concentration experiments using microfiltration (PVDF5, PS5) and ultrafiltration membranes (PES)

VRF	Membrane type	Product	DM (%)	TKN ($g \cdot L^{-1}$) ± SD	TAN ($g \cdot L^{-1}$) ± SD	P ($g \cdot L^{-1}$)	K ($g \cdot L^{-1}$)
0	PVDF5	Concentrate	2.3	3.3 ± 0.06	1.66 ± 0.004	0.148	1.32
0.26	PVDF5	Concentrate	3	3.42 ± 0.13	1.9 ± 0.19	0.173	1.32
0.44	PVDF5	Concentrate	4.4	3.26 ± 0.28	1.79 ± 0.07	0.235	1.30

0.55	PVDF5	Concentrate	4	3.44 ± 0.15	1.94 ± 0.032	0.275	1.37
0	PVDF5	Permeate	1	2.50 ± 0.05	2.69 ± 0.05	0.043	1.16
0.26	PVDF5	Permeate	0.7	2.44 ± 0.10	2.44 ± 0.0	0.046	1.27
0.44	PVDF5	Permeate	1	2.60 ± 0.14	2.59 ± 0.01	0.042	1.23
0.55	PVDF5	Permeate	1	2.51 ± 0.06	2.60 ± 0.01	0.039	1.27
0	PS5	Concentrate	2.5	2.97 ± 0.05	2.64 ± 0.04	0.213	1.47
0.18	PS5	Concentrate	3.4	3.25 ± 0.05	2.68 ± 0.01	0.261	1.53
0.33	PS5	Concentrate	3.9	3.25 ± 0.01	2.7 ± 0.01	0.291	1.40
0.48	PS5	Concentrate	3.9	3.78 ± 0.16	2.81 ± 0.01	0.375	1.53
0	PS5	Permeate	0.8	2.50 ± 0.05	2.69 ± 0.05	0.060	1.37
0.18	PS5	Permeate	0.2	2.44 ± 0.10	2.44 ± 0.0	0.056	1.32
0.33	PS5	Permeate	1.3	2.60 ± 0.14	2.59 ± 0.01	0.059	1.41
0.48	PS5	Permeate	0.9	2.51 ± 0.06	2.60 ± 0.01	0.059	1.41
0	PES	Feed	3.2	nd	2.7	0.53	0.46
0.7	PES	Concentrate	6	nd	2.7	0.45	0.46
0.7	PES	Permeate	0.86	nd	2.8	0.08	0.46

nd – not determined

Table 6: Clean water flux recovery (FR) after basic-acidic cleaning (compared to the clean water flux after membrane flushing)

Membrane type	Flux recovery (%) (at specific operational conditions)			
	1.4 $m \cdot s^{-1}$ and 1.5bar	1.4 $m \cdot s^{-1}$ and 1bar	1.1 $m \cdot s^{-1}$ and 1.5bar	1.1 $m \cdot s^{-1}$ and 1bar
PVDF5	20	7	17	-4
PS5	42	29	12	21

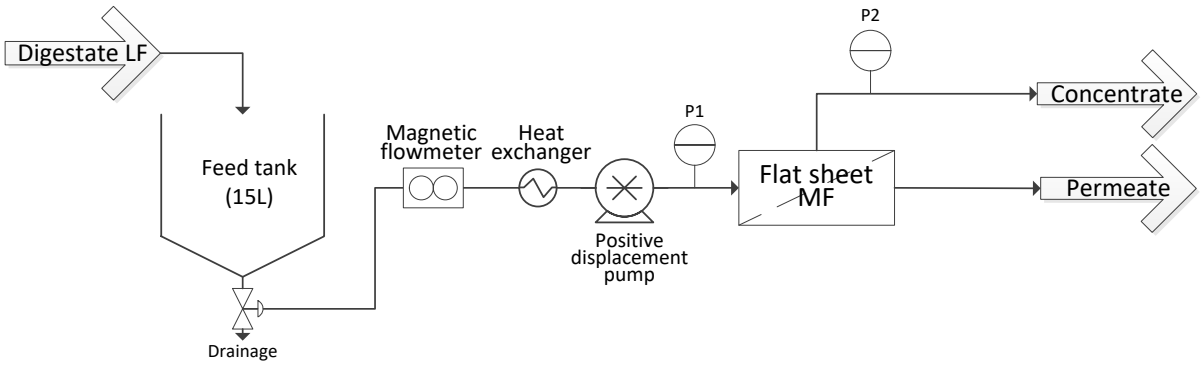

Figure 1: LabStak® microfiltration M10 setup.

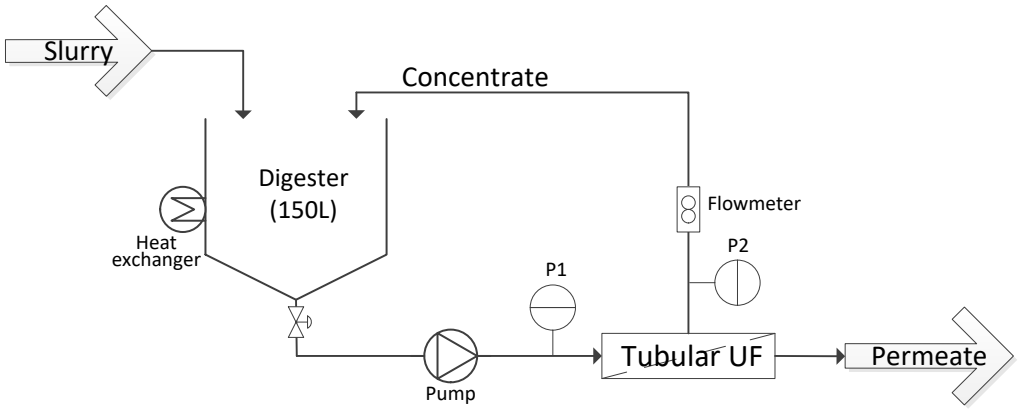

Figure 2: Ultrafiltration pilot plant setup.

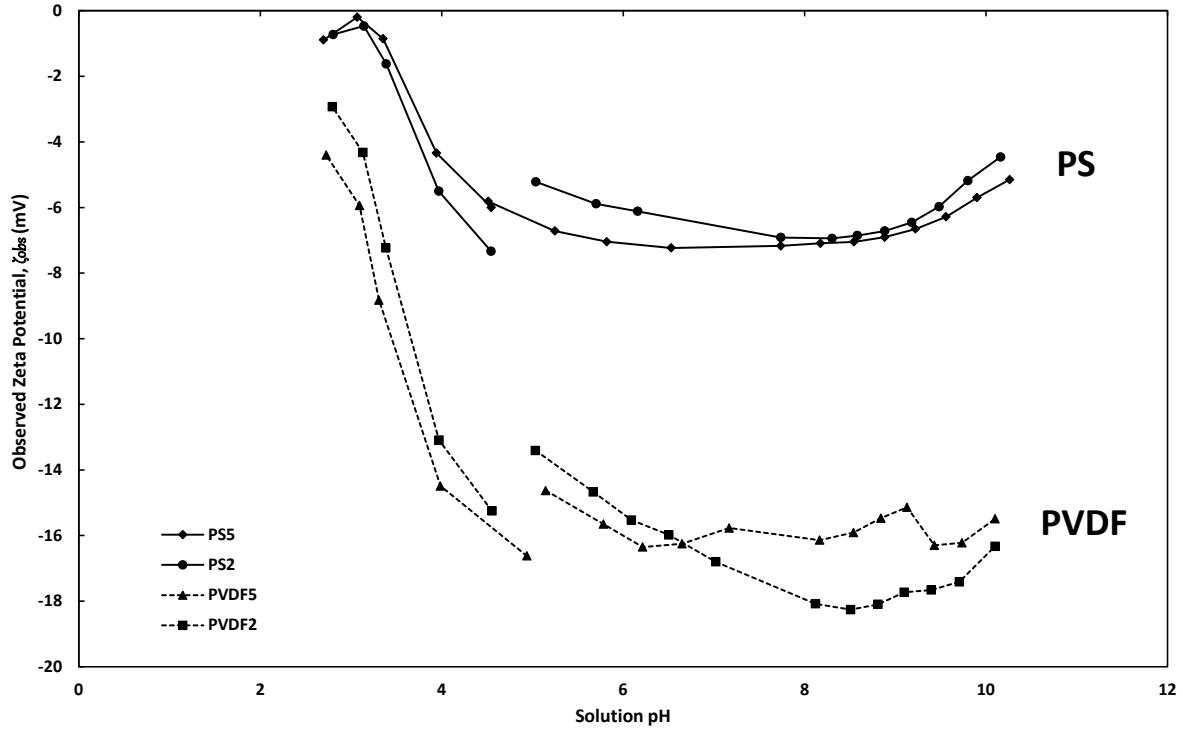

Figure 3: Observed zeta potential as a function of solution pH for PVDF2 and PVDF5, PS2 and PS5 clean membranes (zeta potential calculated as streaming potential per unit of applied pressure on the membrane; each point represents a slope for a linear representation with a correlation better than 0.95).

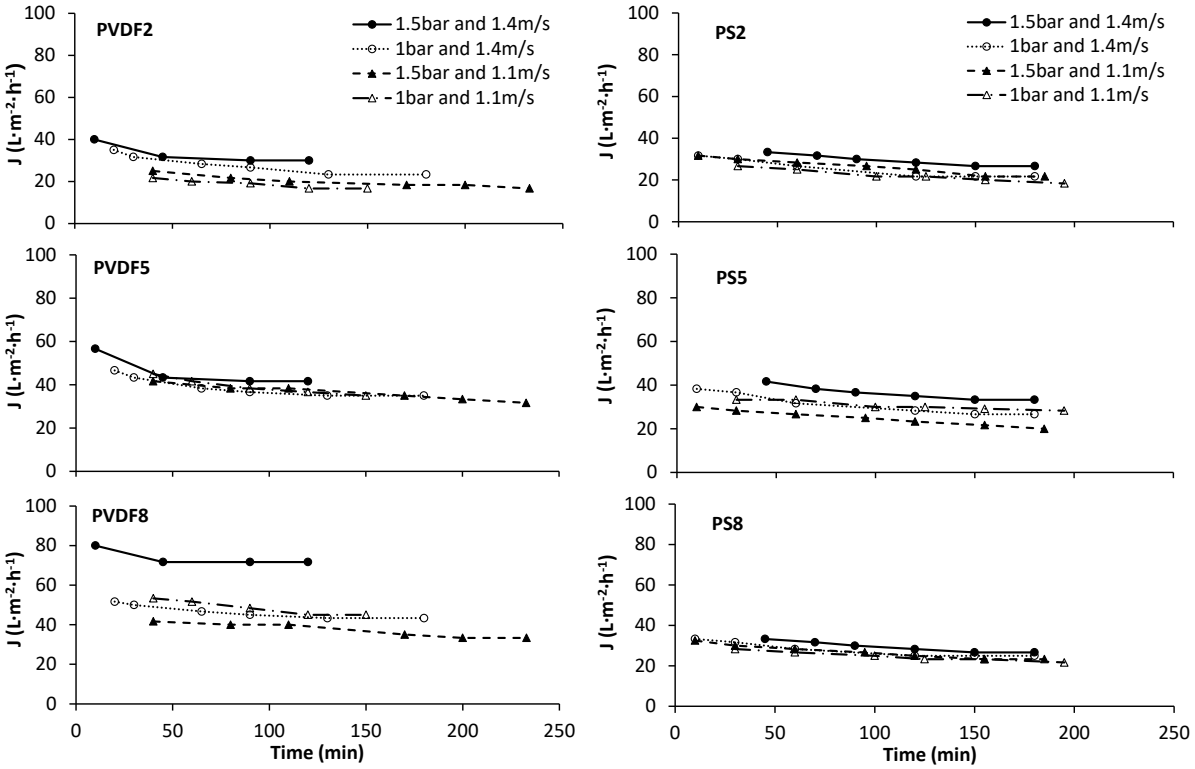

a) b)

Figure 4: a) Permeate flux during microfiltration experiments as a function of operational time using a) PVDF membranes b) PS membranes.

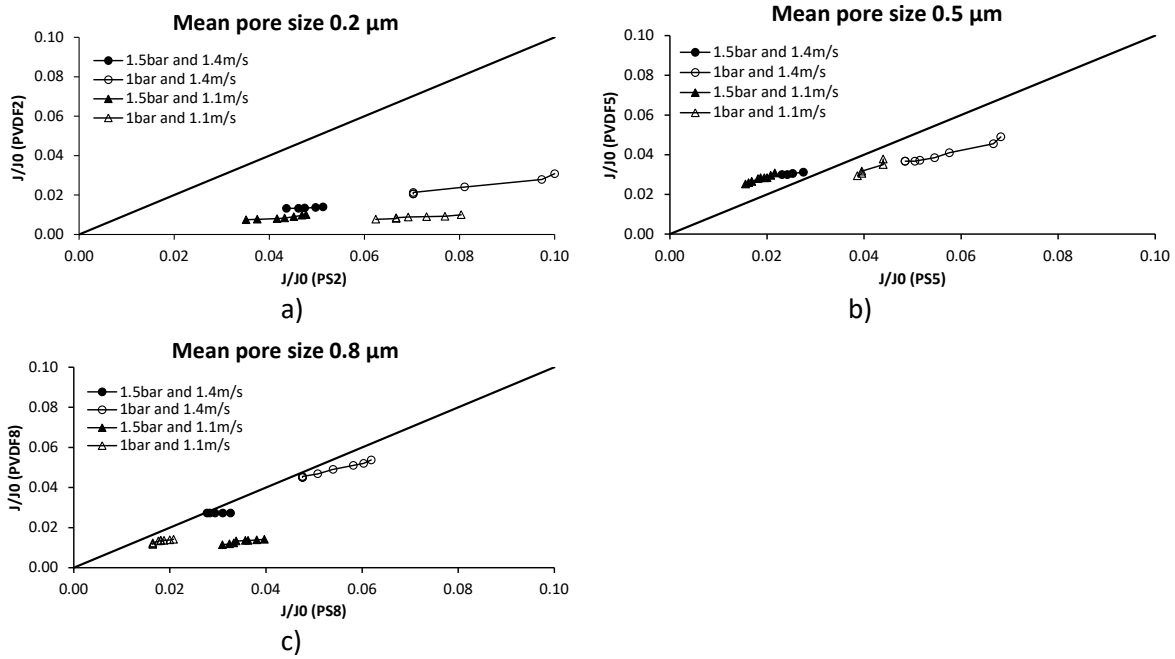

a) b)

c)

Figure 5: Scatter plots for comparison of relative permeate fluxes during microfiltration. Each individual graph stands for comparison of relative permeate flux for a) PVDF2 vs PS2; b) PVDF5 vs PS5; c) PVDF8 vs PS8.

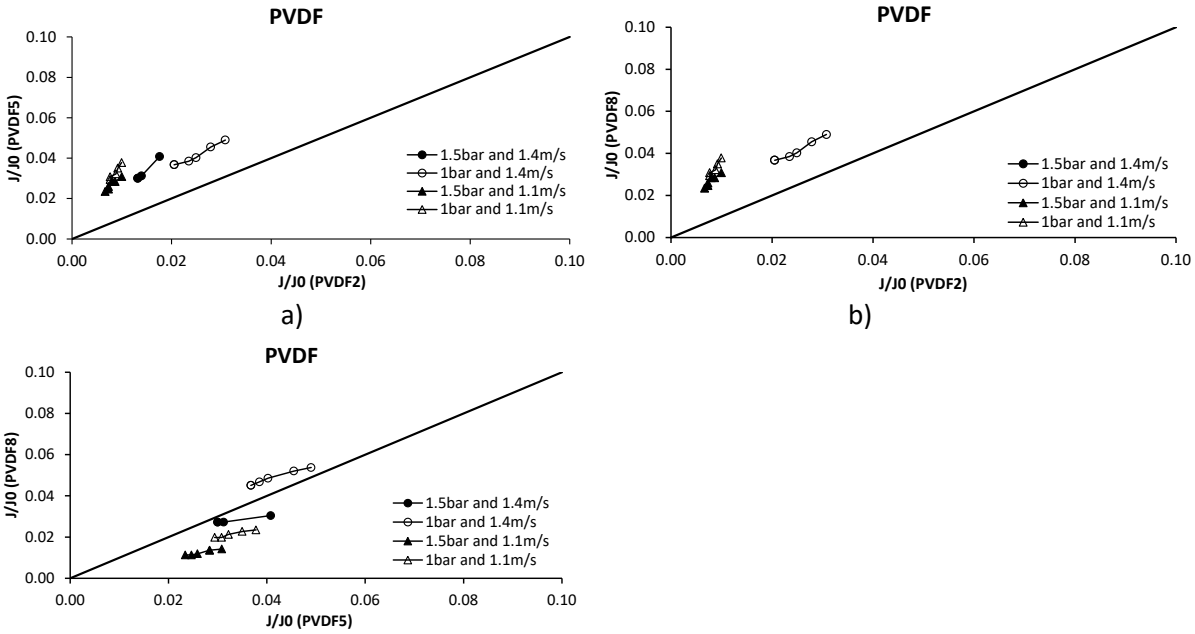

Figure 6: Scatter plots for comparison of relative permeate fluxes during microfiltration considering the influence of pore size within PVDF membranes. Each individual graph stands for comparison of relative flux for a) PVDF5 vs PVDF2; b) PVDF8 vs PVDF2; c) PVDF8 vs PVDF5.

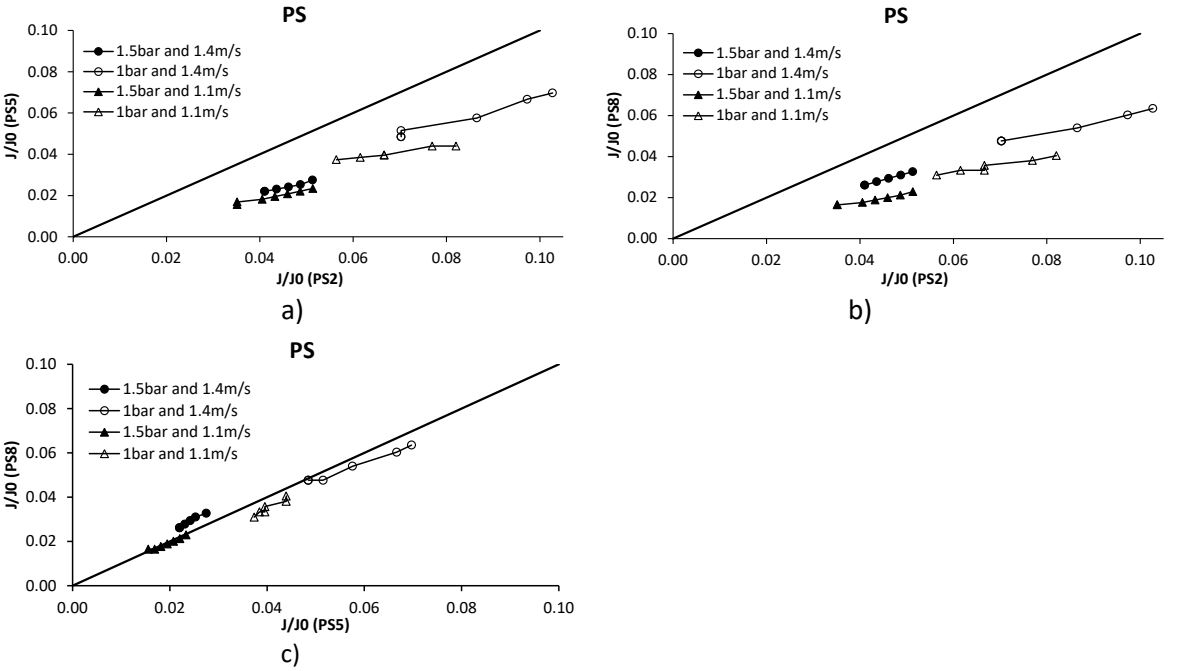

Figure 7: Scatter plots for comparison of relative permeate fluxes during microfiltration considering the considering the influence of pore size within PS membranes. Each individual graph stands for comparison of relative flux for a) PS5 vs PS2; b) PS8 vs PS2; c) PS8 vs PS5.

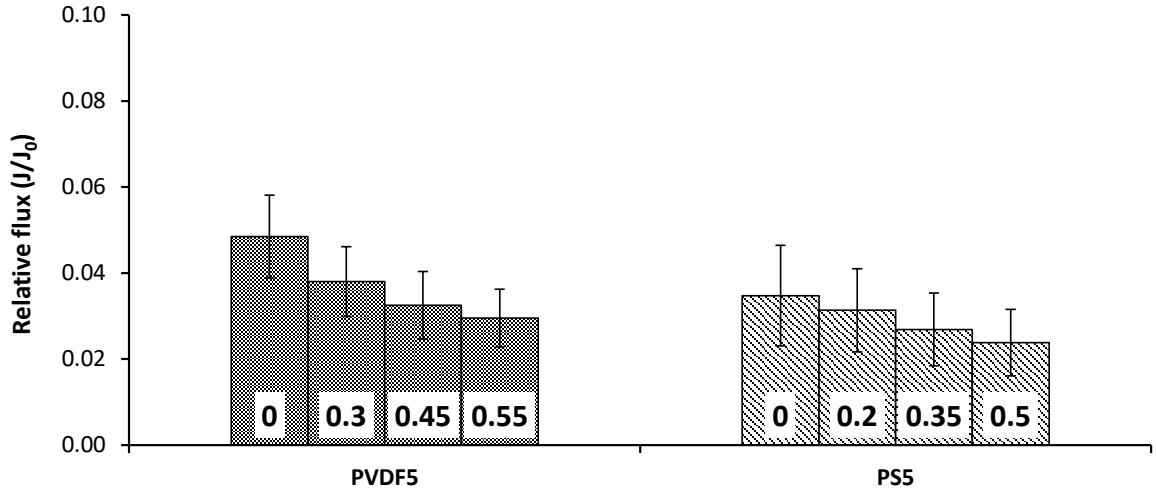

Figure 8: Permeate flux for PVDF5 and PS5 as a function of VRF during microfiltration concentration experiments at 1.4 m·s^{-1} and 1 bar (values inside the column bars indicate the related VRF for each relative flux plotted value).

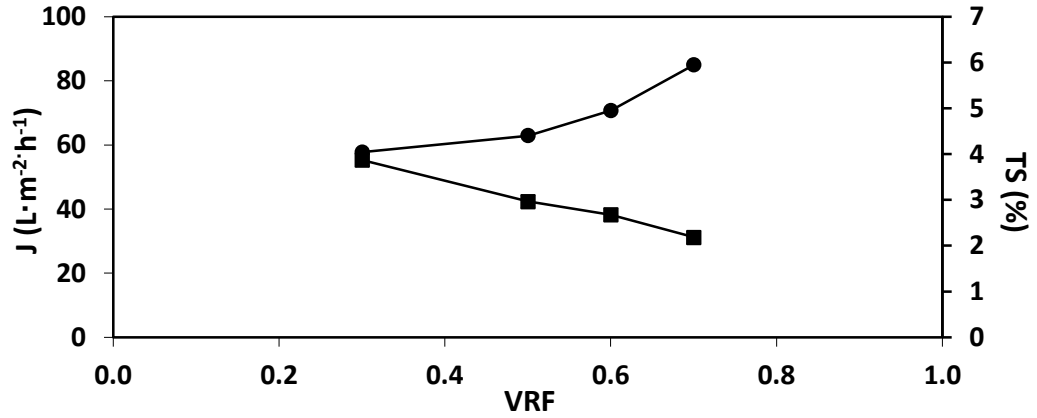

Figure 9: Permeate flux (J) (▪) and DM or total solids-% (•) as a function of volume reduction factor (VRF) during ultrafiltration concentration experiments using PES 40kDa membrane, at 2.6 m·s^{-1} cross flow velocity and transmembrane pressure 2.2 bar.

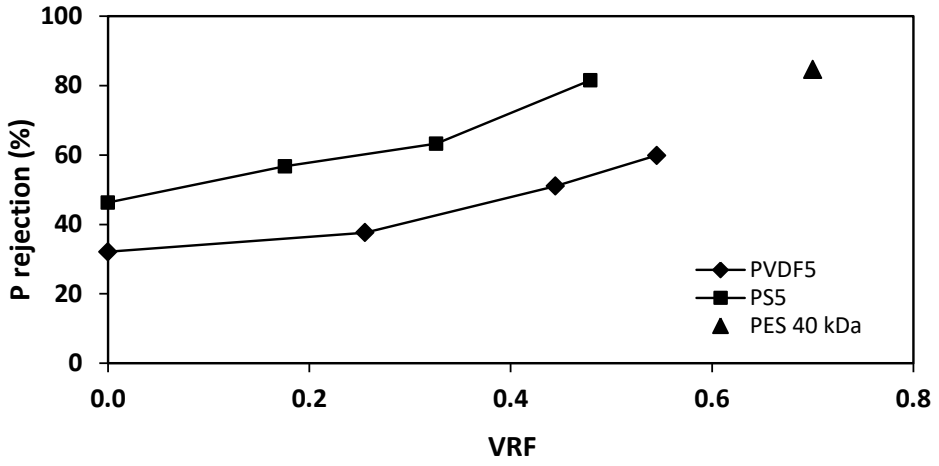

Figure 10: Phosphorus (P) rejection in the concentrate fractions obtained during microfiltration and ultrafiltration concentration experiments

References

[1] M. Hjorth, K.V. Christensen, M.L. Christensen, S.G. Sommer, Solid–liquid separation of animal slurry in theory and practice. A review, Agron. Sustain. Dev, 30 (2010) 153-180.

[2] R. Lopez-Fernandez, C. Aristizabal, R. Irusta, Ultrafiltration as an advanced tertiary treatment of anaerobically digested swine manure liquid fraction: A practical and theoretical study, J Membrane Sci, 375 (2011) 268-275.

[3] J.A. Alburquerque, C. de la Fuente, A. Ferrer-Costa, L. Carrasco, J. Cegarra, M. Abad, M.P. Bernal, Assessment of the fertiliser potential of digestates from farm and agroindustrial residues, Biomass Bioenerg, 40 (2012) 181-189.

[4] O.F. Schoumans, W.H. Rulkens, O. Oenema, P.A.I. Ehlert, Alterra Report 2158 - Phosphorus recovery from animal manure, in: Alterra (Ed.), Wageningen UR, 2010.

[5] C.A.G. Sorensen, S.G. Sommer, D. Bochtis, A. Rotz, M.L. Christensen, T. Schmidt, L.S. Jensen, Technologies and Logistics for Handling, Transport and Distribution of Animal Manures, in: Animal Manure Recycling, Wiley, 2013.

[6] S. Wulf, P. Jager, H. Dohler, Balancing of greenhouse gas emissions and economic efficiency for biogas-production through anaerobic co-fermentation of slurry with organic waste, Agr Ecosyst Environ, 112 (2006) 178-185.

[7] ECC, Directive 2000/60/EC of the European Parliament and of the council of 23 October 2000 establishing a framework for Community action in the field of water policy, in: E. Commission (Ed.) Off. J. European Communities, 2000, pp. 1-72.

[8] J.B. Holm-Nielsen, T. Al Seadi, P. Oleskowicz-Popiel, The future of anaerobic digestion and biogas utilization, Bioresource Technol, 100 (2009) 5478-5484.

[9] L. Masse, D.I. Masse, V. Beaudette, M. Muir, Size distribution and composition of particles in raw and anaerobically digested swine manure, T Asae, 48 (2005) 1943-1949.

[10] F. Waeger, T. Delhaye, W. Fuchs, The use of ceramic microfiltration and ultrafiltration membranes for particle removal from anaerobic digester effluents, Sep Purif Technol, 73 (2010) 271-278.

[11] K.H. Choo, C.H. Lee, U.H. Pek, U.C. Koh, S.W. Kim, J.H. Koh, Characteristics of membrane filtration as a post treatment to anaerobic digestion, J. Korean Ind. Eng. Chem., 3 (1992) 730–738.

563 [12] X. Guo, X. Jin, Treatment of Anaerobically Digested Cattle Manure Wastewater by Tubular
564 Ultrafiltration Membrane, Separ Sci Technol, 48 (2013) 1023-1029.
565 [13] W.R. Ross, J.P. Barnard, J. Le Roux, H.A. De Villiers, Application of ultrafiltration membranes for
566 solids - liquid separation in anaerobic digestion systems: The ADUF process, Water South Africa, 16
567 (1990) 85-91.
568 [14] N.K.H. Strohwald, W.R. Ross, Application of the ADUF process to brewery effluent on a
569 laboratory scale, Water Sci Technol, 26 (1992) 95-105.
570 [15] W.R. Ghyoot, W.H. Verstraete, Coupling membrane filtration to anaerobic primary sludge
571 digestion, Environ Technol, 18 (1997) 569-580.
572 [16] M.L. Gerardo, M.P. Zacharof, R.W. Lovitt, Strategies for the recovery of nutrients and metals
573 from anaerobically digested dairy farm sludge using cross-flow microfiltration, Water research,
574 (2013).
575 [17] B. Wu, Y. An, Y. Li, F.S. Wong, Effect of adsorption/coagulation on membrane fouling in
576 microfiltration process post-treating anaerobic digestion effluent, Desalination, 242 (2009) 183-192.
577 [18] J. Wei, G.S. Helm, N. Corner-Walker, X. Hou, Characterization of a non-fouling ultrafiltration
578 membrane, Desalination, 192 (2006) 252-261.
579 [19] S.P. Beier, A.D. Enevoldsen, G.M. Kontogeorgis, E.B. Hansen, G. Jonsson, Adsorption of Amylase
580 Enzyme on Ultrafiltration Membranes, Langmuir, 23 (2007) 9341-9351.
581 [20] G. Bayramoğlu, E. Yalçin, M.Y. Arica, Adsorption of serum albumin and γ-globulin from single
582 and binary mixture and characterization of pHEMA-based affinity membrane surface by contact
583 angle measurements, Biochemical Engineering Journal, 26 (2005) 12-21.
584 [21] X. Li, Y. Zhang, X. Fu, Adsorption of glutamicum onto polysulphone membrane, Sep Purif
585 Technol, 37 (2004) 187-198.
586 [22] I.H. Huisman, E. Vellenga, G. Trägårdh, C. Trägårdh, The influence of the membrane zeta
587 potential on the critical flux for cross flow microfiltration of particle suspensions, J Membrane Sci,
588 156 (1999) 153-158.
589 [23] N. Lebolay, A. Ricard, Streaming Potential in Membrane Processes - Microfiltration of Egg
590 Proteins, J Colloid Interf Sci, 170 (1995) 154-160.
591 [24] M. Nystrom, M. Lindstrom, E. Matthiasson, Streaming Potential as a Tool in the Characterization
592 of Ultrafiltration Membranes, Colloid Surface, 36 (1989) 297-312.
593 [25] S.S. Deshmukh, A.E. Childress, Zeta potential of commercial RO membranes: influence of source
594 water type and chemistry, Desalination, 140 (2001) 87-95.
595 [26] A. Zarebska, D.R. Nieto, K.V. Christensen, B. Norddahl, Ammonia recovery from agricultural
596 wastes by membrane distillation: Fouling characterization and mechanism, Water research, 56
597 (2014) 1-10.
598 [27] K. Nakamura, T. Orime, K. Matsumoto, Response of zeta potential to cake formation and pore
599 blocking during the microfiltration of latex particles, J Membrane Sci, 401 (2012) 274-281.
600 [28] Anton Paar Instruction Manual - SurPASS Electrokinetic Analyzer, 2009.
601 [29] D.B. Burns, A.L. Zydney, Buffer effects on the zeta potential of ultrafiltration membranes, J
602 Membrane Sci, 172 (2000) 39-48.
603 [30] K. Boussu, B. Van der Bruggen, A. Volodin, C. Van Haesendonck, J.A. Delcour, P. Van der
604 Meeren, C. Vandecasteele, Characterization of commercial nanofiltration membranes and
605 comparison with self-made polyethersulfone membranes, Desalination, 191 (2006) 245-253.
606 [31] A. Martin, F. Martinez, J. Malfeito, L. Palacio, P. Pradanos, A. Hernandez, Zeta potential of
607 membranes as a function of pH - Optimization of isoelectric point evaluation, J Membrane Sci, 213
608 (2003) 225-230.
609 [32] E.W. Rice, R.B. Baird, A.D. Eaton, L.S. Clesceri, Standard methods for the Examination of Water
610 and Wastewater, 22nd ed., American Public Health Association (APHA), American Water Works
611 Association (AWWA), Water Environment Federation (WEF), 2012.
612 [33] E. Arkhangelsky, I. Levitsky, V. Gitis, Electrostatic repulsion as a mechanism in fouling of
613 ultrafiltration membranes, Water Sci Technol, 58.10 (2008) 1955-1961.

614 [34] B. Razi, A. Aroujalian, M. Fathizadeh, Modeling of fouling layer deposition in cross-flow
615 microfiltration during tomato juice clarification, Food Bioprod Process, 90 (2012) 841-848.
616 [35] K.-J. Hwang, C.-Y. Liao, K.-L. Tung, Effect of membrane pore size on the particle fouling in
617 membrane filtration, Desalination, 234 (2008) 16-23.
618 [36] V. Chen, A.G. Fane, S. Madaeni, I.G. Wenten, Particle deposition during membrane filtration of
619 colloids: transition between concentration polarization and cake formation, J Membrane Sci, 125
620 (1997) 109-122.
621